Provably Good Moving Least Squares

Ravikrishna Kolluri *

Abstract

We analyze a *moving least squares* algorithm for reconstructing a surface from point cloud data. Our algorithm defines an implicit function I whose zero set U is the reconstructed surface. We prove that I is a good approximation to the signed distance function of the sampled surface F and that U is geometrically close to and homeomorphic to F. Our proof requires sampling conditions similar to ϵ-sampling, used in Delaunay reconstruction algorithms.

1 Introduction

Point sets have become a popular shape representation as current scanning devices generate dense point sets capable of modeling highly detailed surfaces. These point-based representations have several advantages in modeling and simulation, as mesh topology need not be maintained during surface deformations. However, a continuous definition of the surface represented by the points is needed for some applications such as rendering and resampling. Surface reconstruction algorithms are used to recover these smooth surfaces from point clouds.

The input to our surface reconstruction algorithm is a set S of sample points close to the surface F of a 3D object. Each sample point has an approximate surface normal. The output is an approximation of F. The approximation is represented either implicitly as the zero surface of a scalar function or as a surface triangulation.

Our surface reconstruction algorithm is based on a data interpolation technique called *moving least squares* (MLS). For each sample $s \in S$ we define a globally smooth point function that approximates the signed distance from F in the local neighborhood of s. These functions are then blended together using Gaussian weight functions, yielding a smooth implicit function whose zero set is the reconstructed surface.

Our MLS construction is not new; it was originally proposed by Shen, O'Brien, and Shewchuk [25] for building manifold surfaces from polygon soup. The main contribution of this paper is to introduce theoretical guarantees for MLS algorithms. We prove that the implicit function generated by our algorithm is a good approximation of the signed distance function of the original surface. We also show that the reconstructed surface is geometrically and topologically correct.

The *crust* algorithm of Amenta and Bern [3] was the first surface reconstruction algorithm that guaranteed a correct reconstruction for sufficiently dense sample sets. The crust is defined as a subset of the faces in the Delaunay complex of the sample points. The sampling requirements are defined in terms of *local feature size*, which is the distance from a point on the surface to its closest point on the medial axis. Our sampling conditions, defined in Section 3, are also based on the *local feature size.*

Unlike Delaunay-based algorithms, the MLS surface built by our algorithm might not interpolate the sample points. This allows us to reconstruct smooth surfaces from noisy point clouds. Our algorithm can handle noisy data as long as the amount of noise is small compared to the local feature size of the sample points.

2 Related Work

There has been much work on surface reconstruction from points clouds. A widely used technique defines the reconstructed surface as the zero set of a three-dimensional scalar function built from the input points. Hoppe, DeRose, Duchamp, McDonald, and Stuetzle [16] provide one of the earliest algorithms, which locally estimates the signed distance function induced by the "true" surface being sampled. Curless and Levoy [13] developed an algorithm that is particularly effective for laser range data comprising billions of point samples, like the statue of David reconstructed by the Digital Michelangelo Project [18].

Smooth surfaces can also be built by fitting globally supported basis functions to a point cloud. Turk and O'Brien [26] show that a global smooth approximation can be obtained by fitting radial basis functions. Carr et al. [12] adapt this radial basis function-fitting algorithm to large data sets using multipole expansions.

Instead of computing a single global approximation, moving least squares algorithms locally fit smooth functions to each sample point and blend them together. Ohtake, Belyaev, Alexa, Turk, and Seidel [22] use a partition-of-unity method with a fast hierarchical evaluation scheme to compute surfaces from large data sets. Our MLS construction is based on the algorithm given by Shen, O'Brien, and Shewchuk [25] that introduced the idea of associating functions, rather than just values, with each point to ensure that the gradient of the implicit function matches the gradient of the signed distance function near the sample points.

A different approach to moving least squares is the nonlinear projection method originally proposed by Levin [17]. A point-set surface is defined as the set of stationary points of a projection operator. This surface definition was first used by Alexa et al. [2] for point based modeling and rendering. Since then the surface definition has been used for progressive point-set surfaces [15] and in PointShop3D [24], a point based modeling tool. Amenta and Kil [6] give an

*Department of Computer Science, University of California, Berkeley, Berkeley, CA, 94720. Email: rkolluri@acm.org

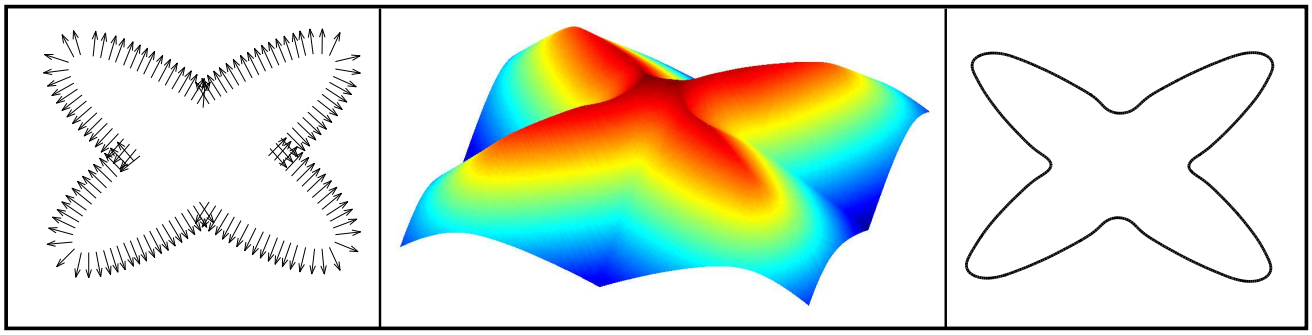

Figure 1: Left, a set of points with outside normals. Center, the implicit function built by our algorithm from the points. Right, the reconstructed curve which is the zero set of the implicit function.

explicit definition of point set surfaces as the local minima of an energy function along the directions given by a vector field. Adamson and Alexa [1] provide a simplified implicit surface definition for efficient ray tracing and define sampling conditions that guarantee a manifold reconstruction. However, current definitions of point-set surfaces come with no guarantees on the correctness of the reconstructed surface.

Following the crust algorithm of Amenta and Bern [3], there have been many Delaunay-based algorithms for surface reconstruction with provable guarantees. Amenta, Choi, Dey, and Leekha [4] present the cocone algorithm, which is much simpler than the crust and prove that the reconstructed surface is homeomorphic to the original surface. The powercrust algorithm of Amenta, Choi, and Kolluri [5] uses weighted Delaunay triangulations to avoid the manifold extraction step of the crust and cocone algorithms. Boissonnat and Cazals [8] build a smooth surface by blending together functions associated with each sample point, using natural neighbor coordinates derived from the Voronoi diagram of the sample points. The robust cocone algorithm of Dey and Goswami [14] guarantees a correct reconstruction for noisy point data. Even when the input points are noisy, surfaces reconstructed by Delaunay algorithms interpolate (a subset of) the sample points. As a result, the reconstructed surface is not smooth and a mesh smoothing step is often necessary.

Smooth meshes that approximate F can by built by contouring the zero set of the implicit function defined by our algorithm. The marching cubes [19] algorithm is widely used for contouring level sets of implicit functions. There has been some recent work on contouring algorithms with theoretical guarantees. Boissonnat and Oudot [11] give a Delaunay-based contouring algorithm that guarantees good quality triangles in the reconstructed surface. Boissonnat, Cohen-Steiner and Vegter [10] present a contouring algorithm with guarantees on the topology of the reconstructed triangulation.

Signed distance functions of surfaces are useful in their own right. Level set methods that have been used in surface reconstruction [27], physical modeling of fluids, and in many other areas rely on signed distance functions to implicitly maintain moving surfaces. See the book by Osher and Fedkiw [23] for an introduction to level set methods. Mitra et al. [20] use approximation of signed distance functions to align overlapping surfaces. The implicit function constructed by our algorithm can be used as an approximation to the signed distance function.

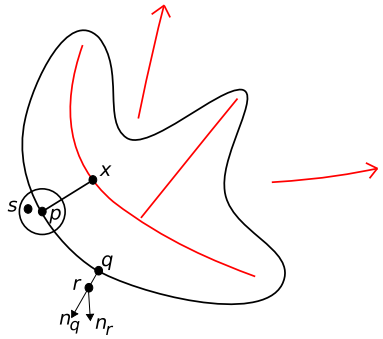

Figure 2: A closed curve along with its medial axis. The local feature size of p is the distance to the closest point x on the medial axis.

3 Sampling Requirements

The *local feature size* (lfs) at a point $p \in F$ is defined as the distance from p to the nearest point of the medial axis of F. A point set S is an ϵ-sample if the distance from any point $p \in F$ to its closest sample in S is less than $\epsilon \mathrm{lfs}(p)$. Amenta and Bern [3] prove that a good approximation to F can be obtained from the Delaunay triangulation of an ϵ-sample S.

Our results on the correctness of the reconstructed surface require *uniform ϵ-sampling*. Assume that the data set has been scaled such that the lfs of any point on F is at least 1. A point set S is a *uniform ϵ-sample* of F if the distance from each point $p \in F$ to its closest sample is less than ϵ. The amount of noise in the samples should be small compared to the sampling density. For each sample s, the distance to its closest surface point p should be less than ϵ^2 as shown in Figure 2. Moreover, the angle between the normal $\vec{n}_r$ of a sample r and the normal $\vec{n}_q$, of the closest surface point to r, should be than ϵ.

Arbitrary oversampling in one region of the surface can distort the value of the implicit function in other parts of the surface. As this rarely happens in practice, we assume that local changes in the sampling density are bounded. Let α_p be the number of samples inside a ball of radius ϵ centered at a point p. We assume that for each point p, if $\alpha_p > 0$, the number of samples inside a ball at radius 2ϵ at p is at most 8α. We will use two parameters to state our geometric results. The value of ϵ depends on the sampling density and we define a second parameter, $\tau = 2\epsilon$. The results in this paper hold true for values of $\epsilon \leq 0.01$.

4 Surface Definition

Given a set of sample points S near a smooth, closed surface F, our algorithm builds an implicit function I whose zero surface U approximates F. We assume that the outside surface normal $\vec{n}_i$ is approximately known for each sample point $s_i \in S$ as shown in Figure 1. In practice, the normal of s_i is obtained by local least squares fitting of a plane to the samples in the neighborhood around s_i. Mitra, Nguyen and Guibas [21] analyze the least squares method for normal estimation and present an algorithm for choosing an optimal neighborhood around each sample point.

Our algorithm begins by constructing a point function for each sample point in S. The point function P_{s_i} for sample point s_i is defined as the signed distance function from x to the tangent plane at s_i, $P_{s_i}(x) = (x - s_i) \cdot \vec{n}_i$.

The implicit function I is a weighted average of the point functions.

$$I(x) = \frac{\sum_{s_i \in S} W_i(x)((x - s_i) \cdot \vec{n}_i)}{\sum_{s_j \in S} W_j(x)}.$$

We use Gaussian functions, $W_i(x) = e^{-\|x-s_i\|^2/\epsilon^2}/A_i$ in computing the weighted average of the point functions. Here A_i is the number of samples inside a ball of radius ϵ centered at s_i, including s_i itself.

5 Geometric Properties

Amenta and Bern [3] prove the following Lipschitz condition on the surface normal with respect to the *local feature size*. As we assume that for each point $p \in F$, $\mathrm{lfs}(p) \geq 1$, we can state the Lipschitz condition in terms of the distance between two points.

Theorem 1. *For points p, q on the surface F with $d(p, q) \leq r$, for any $r < 1/3$, the angle between the normals at p and q is at most $r/(1 - 3r)$ radians.*

Consider the surface inside a small ball B centered at a point $p \in F$. As shown in Figure 3, the surface inside B has to be outside the medial balls at p. As a result, the surface inside B lies between two planes close to the tangent plane of p.

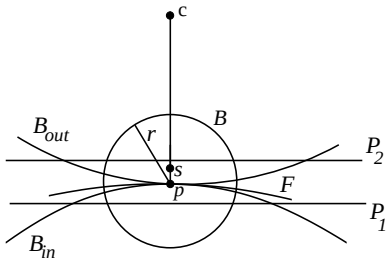

Figure 3: The surface inside a ball B of radius r has to be outside the medial balls B_i and B_o. As a result, all samples in B are between two planes P_1 and P_2 that are at a distance of $O(r^2 + \epsilon^2)$ from p.

Observation 2. *For a point $p \in F$, let B be a ball of radius $r < 0.1$ centered at p. The samples inside B lie between two planes P_1, P_2 parallel to the tangent plane at p. The distance from p to P_1, P_2 is less than $\frac{(r+\epsilon^2)^2}{2} + \epsilon^2$.*

Let F_{out} be the outside τ-offset surface of F that is obtained by moving each point x on F along the normal at x by a distance τ. Similarly, let F_{in} be the inside τ-offset surface of F. The τ-neighborhood is the region bounded by the inside and the outside offset surfaces. For any point x inside the τ-neighborhood, $|\phi(x)| < \tau$, where ϕ is the signed distance function of F.

The main result in this section is that the zero set U is geometrically close to F. We show this by proving that U is inside the τ-neighborhood of F (Theorem 9). We then show that the reconstructed surface is a manifold by proving that the gradient of I is non-zero at each point in the zero set of I(Theorem 18).

Consider a point x shown in Figure 4, whose closest point on the surface is p. The vector $\vec{xp}$ is parallel to the surface normal of p and $\|\vec{xp}\| = |\phi(x)|$. Let $B_1(x), B_2(x)$ be two balls centered at point x. The radius of $B_1(x)$ is $|\phi(x)|$ and $B_2(x)$ is a slightly larger ball whose radius is $|\phi(x)| + \tau + \epsilon$.

Let $N(x)$ be the weighted combination of the point functions at x, $N(x) = \sum_{s_i \in S} W_i(x) P_{s_i}(x)$ and let $D(x)$ be the sum of all weight functions at x, $D(x) = \sum_{s_i \in S} W_i(x)$

Our geometric results are based on the observation that samples outside $B_2(x)$ have little effect on the value of the implicit function at x. To see this, we first separate the contributions of samples inside $B_2(x)$ and samples outside $B_2(x)$. Let $N_{\text{in}}(x) = \sum_{s_i \in B_2(x)} W_i(x) P_{s_i}(x)$ and $N_{\text{out}}(x) = \sum_{s_i \notin B_2(x)} W_i(x) P_{s_i}(x)$ be the contributions to $N(x)$ by samples inside and outside $B_2(x)$. Similarly, let $D_{\text{in}}(x) = \sum_{s_i \in B_2(x)} W_i(x)$ and $D_{\text{out}}(x) = \sum_{s_i \notin B_2(x)} W_i(x)$ be the contributions to $D(x)$ by samples inside and outside $B_2(x)$.

Consider the space outside $B_2(x)$ divided into spherical shells of width ϵ as shown in Figure 4. Let H_w be the region between balls of radius w and $w + \epsilon$. We bound the contributions of all samples outside $B_2(x)$ by summing over the contributions of all samples in each shell.

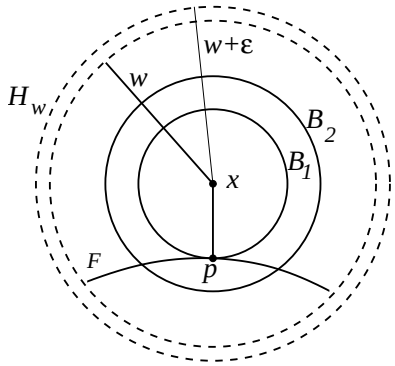

Figure 4: For a point x, p is the closest point to x on the surface. The space outside the ball $B_2(x)$ is divided into spherical shells of width ϵ. H_w is the shell bounded by spheres of radius w and $w+\epsilon$.

We begin by proving an upper bound on the number of samples inside each shell normalized by their oversampling factors.

Lemma 3. *For a ball B_ϵ of radius $\frac{\epsilon}{2}$, $\sum_{s_i \in B_\epsilon} \frac{1}{A_i} \leq 1$.*

Proof. If B_ϵ is empty we are done; assume that B_ϵ contains $\alpha > 0$ samples. Let s_i be a sample inside B_ϵ. As all samples inside B_ϵ are inside a ball of radius ϵ centered at s_i, $A_i \geq \alpha$. Hence the contribution of all samples inside B_ϵ is given by $\sum_{s_i \in B_\epsilon} \frac{1}{A_i} \leq \alpha \frac{1}{\alpha} \leq 1$. □

Lemma 4. *For samples s_i in spherical shell H_w centered at point x,*

$$\sum_{s_i \in H_w} \frac{1}{A_i} < \frac{200}{\epsilon^2}(w^2 + w\epsilon + \epsilon^2).$$

Proof. Let C be the smallest number of spheres of radius $\frac{\epsilon}{2}$ that cover H_w. Consider a covering of H_w with axis-parallel cubes of size $\frac{\epsilon}{\sqrt{3}}$. Any cube that intersects H_w is inside a slightly larger shell bounded by spheres of radius $w+2\epsilon$ and $w-\epsilon$ centered at x. So the number of cubes that cover H_w is less than $\frac{36\sqrt{3}\pi\epsilon(w^2+w\epsilon+\epsilon^2)}{\epsilon^3}$. Any cube in this grid is covered by a sphere of radius $\frac{\epsilon}{2}$. Applying Lemma 3 to each sphere, $\sum_{s_i \in H_w} \frac{1}{A_i} \leq C \leq \frac{36\sqrt{3}\pi\epsilon(w^2+w\epsilon+\epsilon^2)}{\epsilon^3} < \frac{200}{\epsilon^2}(w^2 + w\epsilon + \epsilon^2)$. □

5.1 Offset Regions. In this section we obtain bounds on the difference between $I(x)$ and the signed distance function $\phi(x)$ for points x outside the τ-neighborhood and use these bounds to show that the implicit function is non-zero outside the τ-neighborhood.

We begin with a result about the point functions of samples inside $B_2(x)$. We prove that for any sample $s \in B_2(x)$, $P_s(x)$ is close to $\phi(x)$. In order to state this result for points in the inside and outside offset regions, it is convenient to define $\mu(x) = \frac{\phi(x)}{|\phi(x)|}$ to be the sign function of F. For x outside F_{out}, $\mu(x) = 1$ and for x inside F_{in}, $\mu(x) = -1$.

Lemma 5. *Let x be a point outside the τ-neighborhood. Let $P_s(x)$ be the point function of sample $s \in B_2(x)$, evaluated at x. Then,*

$$\mu(x)P_s(x) \leq \mu(x)\phi(x) + 3\epsilon,$$

and,

$$\mu(x)P_s(x) \geq \mu(x)\phi(x)(1-6\epsilon) - 12\epsilon^2.$$

Proof. Let p be the closest point to x on the surface. Then, $d(x,p) = \mu(x)\phi(x)$. Recall that $\tau = 2\epsilon$. As $s \in B_2(x)$,

$$\begin{aligned} \mu(x)P_s(x) &\leq d(x,s) \\ &\leq d(x,p) + \tau + \epsilon \\ &< \mu(x)\phi(x) + 3\epsilon. \end{aligned}$$

Let p' be the closest point to s on the surface F as shown in Figure 5. Let B_m be the medial ball touching p' on the side of F opposite x and let l be the radius of B_m. Let θ be the angle between xp' and the normal at p'. The distance between x and the center of B_m is given by,

$$d^2(x,q) = (d(x,p')\cos\theta + l)^2 + d^2(x,p')\sin^2\theta.$$

The medial ball B_m cannot intersect $B_1(x)$ which is contained in a medial ball on the opposite side of the surface. Hence the sum of their radii should be less than the distance between their centers.

$$\begin{aligned} (l + d(x,p))^2 &\leq (d(x,p')\cos\theta + l)^2 \\ &\quad + d^2(x,p')\sin^2\theta. \\ \cos\theta &\geq \frac{2ld(x,p) - (d^2(x,p') - d^2(x,p))}{2ld(x,p')}. \end{aligned}$$

From the sampling conditions, $d(x,s) \geq d(x,p') - \epsilon^2$ and the angle between the normal at s and the surface normal at p' is less than ϵ. As $d(x,p') \geq \tau$, the angle between xs and xp' is less than $\arcsin(\frac{\epsilon^2}{\tau}) < \frac{2\epsilon^2}{\tau}$. So the angle between xs and the normal at s is at most $\theta + \frac{2\epsilon^2}{\tau} + \epsilon$. Using standard trigonometric formulae, it is easy to show that, $\cos(\theta + \frac{2\epsilon^2}{\tau} + \epsilon) \geq \cos\theta - \frac{2\epsilon^2}{\tau} - \epsilon$.

$$\begin{aligned} \mu(x)P_s(x) &\geq d(x,s)\cos(\theta + \frac{2\epsilon^2}{\tau} + \epsilon) \\ &\geq (d(x,p') - \epsilon^2) \cdot \\ &\quad \left(\frac{2ld(x,p) - (d^2(x,p') - d^2(x,p))}{2ld(x,p')} \right. \\ &\quad \left. - \frac{2\epsilon^2}{\tau} - \epsilon \right). \end{aligned}$$

From the local feature size assumption, $l \geq 1$. Substituting the value of $\tau = 2\epsilon$ we have,

$$\mu(x)P_s(x) \geq \mu(x)\phi(x)(1-6\epsilon) - 12\epsilon^2.$$ □

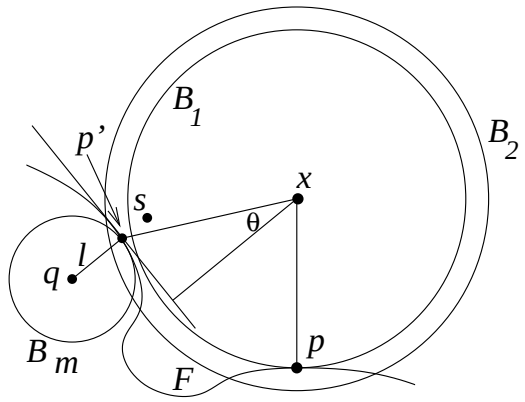

Figure 5: Sample s is inside $B_2(x)$ and p' is the point closest to s on F. B_m is a medial ball touching p' on the side of F opposite x.

Using the result of Lemma 5, it is easy to show that for each sample $s \in B_2(x)$, $P_s(x)$ and $\phi(x)$ are either both positive or both negative.

Corollary 6. *Let x be a point outside the τ-neighborhood. For a sample $s \in B_2(x)$, let $P_s(x)$ be the point function of s evaluated at x. For values of $\epsilon \leq 0.08$, $\phi(x)P_s(x) > 0$.*

Proof. For a point x outside F_{out}, $\phi(x) \geq \tau \geq 2\epsilon$. Applying the lower bound on $P_S(x)$ from Lemma 5, we can write

$$\phi(x)P_s(x) \geq 2\epsilon(2\epsilon(1-6\epsilon) - 12\epsilon^2).$$

It is now easy to check that for $\epsilon \leq 0.08$, $2\epsilon(1-6\epsilon) - 12\epsilon^2 > 0$. A similar argument proves the result for points inside F_{in}. □

We now prove two results showing that the points outside $B_2(x)$ have little effect on the value of $I(x)$. In Lemma 7 we prove that $D_{\text{out}}(x) \ll D_{\text{in}}(x)$ and in Lemma 8 we prove that $|N_{\text{out}}(x)| \ll |N_{\text{in}}(x)|$. We will use two constants $c_1 = 0.05$ and $c_2 = 0.01c_1$ to state our geometric results.

Lemma 7. *Let x be a point outside the τ-neighborhood. Let $D_{\text{out}}(x)$ and $D_{\text{in}}(x)$ be the total weights of samples inside $B_2(x)$ and outside $B_2(x)$ at x, respectively. Then, $\frac{D_{\text{out}}(x)}{D_{\text{in}}(x)} < c_1$.*

Proof. Consider the division of space outside $B_2(x)$ into spherical shells of width ϵ starting with $B_2(x)$ whose radius is $w_0 = |\phi(x)| + \tau + \epsilon$, as shown in Figure 4. The value of the Gaussian function associated with each sample inside shell H_w at x is at most e^{-w^2/ϵ^2}. Using the bound on the weight of samples in H_w from Lemma 4,

$$\begin{aligned} D_{\text{out}}(x) &\leq \frac{200}{\epsilon^2}\sum_{i=0}^{\infty}(w_i^2 + \epsilon w_i + \epsilon^2)e^{-w_i^2/\epsilon^2} \\ &\leq \frac{200}{\epsilon^2}\sum_{i=0}^{\infty}(w_i^2 + \epsilon w_i + \epsilon^2)e^{-(w_0 w_i)/\epsilon^2}. \quad (1) \end{aligned}$$

Here w_i=$w_0 + i\epsilon$ is the radius of the smaller sphere bounding the i^{th} shell. The dominant term in Equation 1 is a geometric series with a common ratio $e^{-w_0/\epsilon} < 0.01$. The summation has a closed form solution easily obtained using Mathematica. An upper bound is given by

$$D_{\text{out}}(x) \leq \frac{400}{\epsilon^2}(w_0^2 + \epsilon w_0 + \epsilon^2)e^{-w_0^2/\epsilon^2}.$$

We now obtain a lower bound on the contribution of samples inside $B_2(x)$. Let B_ϵ be a ball of radius ϵ centered at p. From the sampling conditions, we know that B_ϵ contains $\alpha \geq 1$ samples. In our sampling requirements, we also assumed that the rate of change in sampling density is bounded. Since a ball of radius ϵ centered at p contains $\alpha \geq 1$ samples, a ball of radius 2ϵ centered at p contains at most 8α samples. So the normalizing factor associated with $s_i \in B_\epsilon$, $\frac{1}{A_i} \geq \frac{1}{8\alpha}$. We now have a lower bound on the weight of samples inside B_ϵ:

$$\begin{aligned} D_{\text{in}}(x) &\geq \sum_{s_i \in B_\epsilon}\frac{1}{A_i}e^{-(|\phi(x)|+\epsilon)^2/\epsilon^2} \\ &\geq \frac{\alpha}{8\alpha}e^{-(|\phi(x)|+\epsilon)^2/\epsilon^2} \\ &= \frac{1}{8}e^{-(|\phi(x)|+\epsilon)^2/\epsilon^2}. \quad (2) \end{aligned}$$

An upper bound on the ratio of the inside and the outside weights is given by,

$$\begin{aligned} \frac{D_{\text{out}}(x)}{D_{\text{in}}(x)} &\leq \frac{3200}{\epsilon^2}(w_0^2 + \epsilon w_0 + \epsilon^2)e^{-(w_0^2 - (|\phi(x)|+\epsilon)^2)/\epsilon^2} \quad (3) \\ &= \frac{3200}{\epsilon^2}(w_0^2 + \epsilon w_0 + \epsilon^2)e^{-\tau(2|\phi(x)|+\tau+2\epsilon)/\epsilon^2}. \end{aligned}$$

For $|\phi(x)| \geq \tau$, $\frac{D_{\text{out}}(x)}{D_{\text{in}}(x)}$ is a monotonically decreasing function of $|\phi(x)|$. The maximum value is obtained for $|\phi(x)| = \tau$ and $w_0 = 2\tau + \epsilon = 5\epsilon$.

$$\frac{D_{\text{out}}(x)}{D_{\text{in}}(x)} \leq \frac{3200}{\epsilon^2}(31\epsilon^2)e^{-16} < c_1. \qquad \square$$

Using the proof technique of Lemma 7 we now prove that $\frac{|N_{\text{out}}(x)|}{|N_{\text{in}}(x)|}$ is very small.

Lemma 8. *Let x be a point outside the τ-neighborhood. Let $N_{\text{out}}(x)$ and $N_{\text{in}}(x)$ be the contributions of samples inside $B_2(x)$ and outside $B_2(x)$ to $N(x)$, respectively. Then, $\frac{|N_{\text{out}}|}{|N_{\text{in}}|} < c_1$.*

Proof. To compute an upper bound for $N_{\text{out}}(x)$, again consider the space outside $B_2(x)$ divided into shells of radius ϵ as shown in Figure 4. For $w \geq \tau$, the value of we^{-w^2/ϵ^2} decreases as w increases. Hence for a sample s_i inside the shell H_w, $|P_{s_i}(x)|W_i(x) \leq \frac{we^{-w^2/\epsilon^2}}{A_i}$. Let $w_0 = |\phi(x)| + \tau + \epsilon$ and $w_i = w_0 + i\epsilon$. Using the bound on

the weight of samples in H_w from Lemma 4,

$$\begin{aligned} |N_{\text{out}}(x)| &\leq \frac{200}{\epsilon^2}\sum_{i=0}^{\infty}(w_i^2+\epsilon w_i+\epsilon^2)w_i e^{-w_i^2/\epsilon^2} \\ &\leq \frac{200}{\epsilon^2}\sum_{i=0}^{\infty}(w_i^2+\epsilon w_i+\epsilon^2)w_i e^{-(w_0 w_i)/\epsilon^2}. \end{aligned}$$

Like the summation in Equation 1, the above summation has a closed form solution easily obtained using Mathematica.

$$|N_{\text{out}}(x)| < \frac{400}{\epsilon^2}w_0(w_0^2+\epsilon w_0+\epsilon^2)e^{-w_0^2/\epsilon^2}.$$

From Corollary 6, the point functions of all samples inside $B_2(x)$ have the same sign at x. Hence a lower bound on the contribution of the sample points inside $B_2(x)$ to $|N_{\text{in}}(x)|$ is given by summing over the contributions of all samples inside a ball B_ϵ of radius ϵ around p.

$$|N_{\text{in}}(x)| \geq \min_{s_i \in B_\epsilon(x)}\{|P_{s_i}(x)|\}D_{\text{in}}(x).$$

From Theorem 1, the angle between the normal of each sample $s_i \in B_\epsilon(x)$ and the normal of p is at most 2ϵ. As x is outside the τ-neighborhood, $|P_{s_i}(x)| \geq \tau\cos 2\epsilon$. Substituting the lower bound of $D_{\text{in}}(x)$ from Equation 2,

$$|N_{\text{in}}(x)| > \frac{\tau}{10}e^{-(|\phi(x)|+\epsilon)^2/\epsilon^2}.$$

$$\begin{aligned} \frac{|N_{\text{out}}(x)|}{|N_{\text{in}}(x)|} &\leq \frac{4000}{\epsilon^2\tau}w_0(w_0^2+\epsilon w_0+\epsilon^2)e^{-(w_0^2-(|\phi(x)|+\epsilon)^2)/\epsilon^2} \\ &\leq \frac{4000}{\epsilon^2\tau}w_0(w_0^2+\epsilon w_0+\epsilon^2)e^{-\tau(2|\phi(x)|+\tau+2\epsilon)/\epsilon^2}. \end{aligned}$$

The value of $\frac{N_{\text{out}}(x)}{N_{\text{in}}(x)}$ is smallest for $|\phi(x)|=\tau$. Substituting the value of $\tau = 2\epsilon$,

$$\frac{|N_{\text{out}}(x)|}{|N_{\text{in}}(x)|} \leq \frac{4000}{2\epsilon^3}(135\epsilon^3)e^{-16} < c_1. \qquad \square$$

Lemma 8 proves that $I(x)$ is mostly determined by the point functions of the samples inside the ball $B_2(x)$. We can derive bounds for $I(x)$ in terms of $\phi(x)$ by combining the results in Lemma 8 and Lemma 5.

$$\mu(x)I(x) \leq (\mu(x)\phi(x)+3\epsilon)(1+c_1). \qquad (4)$$

We can also derive a similar lower bound on $I(x)$.

$$\mu(x)I(x) \geq (\mu(x)\phi(x)(1-6\epsilon)-12\epsilon^2)\frac{1-c_1}{1+c_1}. \qquad (5)$$

Equation 4 and Equation 5 show that the implicit function is close to the signed distance function for points outside the τ-neighborhood. We now have all the tools required to prove our main geometric result: the implicit function $I(x)$ is non-zero outside the τ-neighborhood.

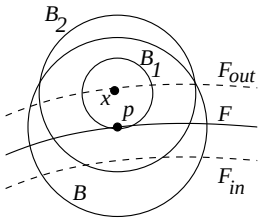

Figure 6: For x in the τ-neighborhood, the samples inside balls $B_1(x)$ and $B_2(x)$ are inside a ball of radius 6ϵ centered at p.

Theorem 9. *Let $\epsilon \leq 0.08$. For each point x outside F_{out}, $I(x) > 0$ and for each point y inside F_{in}, $I(y) < 0$.*

Proof. This proof is exactly like the proof of Corollary 6. It is easier to get the result directly from Equation 5. Consider a point x outside F_{out}. From Equation 5,

$$\begin{aligned} I(x) &\geq (\mu(x)\phi(x)(1-6\epsilon)-12\epsilon^2)\frac{1-c_1}{1+c_1} \\ &\geq (2\epsilon(1-6\epsilon)-12\epsilon^2)\frac{1-c_1}{1+c_1}. \end{aligned}$$

For $\epsilon \leq 0.08$, it is easy to check that $2\epsilon(1-6\epsilon)-12\epsilon^2 > 0$. A similar argument proves that the implicit function is negative at any point inside F_{in}. $\square$

Theorem 9 proves that the implicit function I does not have any spurious zero crossings far away from the sample points. We now have an upper bound of τ on the Hausdorff distance between F and U.

Theorem 10. *For a point $x \in U$, let p be the closest point in F. Then $d(x,p) \leq \tau$.*

Proof. From Theorem 9, the implicit function has a non-zero value outside the τ-neighborhood. Hence, the point x is constrained to lie inside the τ-neighborhood of F and $d(x,p) \leq \tau$. $\square$

Theorem 11. *For a point $p \in F$, let x be the closest point in U. Then, $d(x,p) \leq \tau$.*

Proof. If $I(p) = 0$ we are done; assume without loss of generality that $I(p) < 0$. Let q be the closest point to p on the outside offset surface F_{out}. From Theorem 9, $I(q) > 0$. As the implicit function I is continuous, there is a point y on pq at which $I(y) = 0$ and $d(y,p) \leq \tau$. Since x is the closest point to p in U, $d(x,p) \leq d(y,p) \leq \tau$. $\square$

5.2 The τ-neighborhood. To guarantee that U is a manifold, we have to prove that the gradient of I is non-zero at each point in U. We know from the results in Section 5.1 that U is inside the τ-neighborhood of F. In this section we will study the properties of $\nabla I(x)$ for points x inside the τ-neighborhood.

For a point x inside the τ-neighborhood, $B_2(x)$ is defined as a ball of radius $\sqrt{(|\phi(x)|+\epsilon)^2+25\epsilon^2}$ centered at x. With this new definition of $B_2(x)$, it is easy to show that the samples inside $B_2(x)$ are contained in a small ball centered at the point closest to x in F.

Observation 12. *Let x be a point that is inside the τ-neighborhood as shown in Figure 6. Let p be the closest point to x in F. All samples inside $B_2(x)$ are contained in a ball of radius 6ϵ centered at p.*

Because of the Lipschitz condition on the surface normals of F, the difference between the point functions of the samples inside a small ball at a point on the surface is bounded.

Lemma 13. *Consider a point x whose closest point on the surface F is p. Let $\vec{n}$ be the surface normal at p and let B be a ball of radius 6ϵ at p. For each sample $s_i \in B$, $P_{s_i}(x) = \phi(x) + \zeta_i$ where $|\zeta_i| \leq 56\epsilon^2 + 36|\phi(x)|\epsilon^2$.*

Proof. Let p_i be the closest point to s_i on the surface. As $d(p,p_i) \leq 6\epsilon+\epsilon^2$, the angle between the normal at p_i and $\vec{n}$ is less than $\frac{6\epsilon+\epsilon^2}{1-3(6\epsilon+\epsilon^2)}$ from Theorem 1. Let $\vec{n_i}$ be the normal associated with s_i. From the sampling conditions the angle between the normal of p_i and $\vec{n_i}$ is at most ϵ. So the angle between $\vec{n_i}$ and $\vec{n}$ is given by, $\theta < \frac{6\epsilon+\epsilon^2}{1-3(6\epsilon+\epsilon^2)} + \epsilon$. We can now write $\vec{n_i} = \vec{n} + \vec{\delta_i}$, where $\|\vec{\delta_i}\| \leq \frac{\theta}{\sqrt{2}}$.

$$\begin{aligned}(x-s_i)\cdot\vec{n_i} &= ((x-p)+(p-s_i))\cdot\vec{n_i}\\ &= (x-p)\cdot\vec{n_i} + (p-s_i)\cdot(\vec{n}+\vec{\delta_i})\\ &= (x-p)\cdot\vec{n} - (x-p)\cdot(\vec{n}-\vec{n_i})\\ &\quad +(p-s_i)\cdot(\vec{n}+\vec{\delta_i}).\end{aligned}$$

Because p is the closest point to x on the surface, $(x-p)\cdot\vec{n} = \phi(x)$ and $(x-p)$ is parallel to $\vec{n}$. Since the angle between $\vec{n}$ and $\vec{n_i}$ is less than θ,

$$|(x-p)\cdot(\vec{n}-\vec{n_i})| \leq |\phi(x)|(1-\cos\theta) \leq \frac{|\phi(x)|\theta^2}{2}.$$

Since sample s_i is inside B,

$$|(p-s_i)\cdot\vec{\delta_i}| \leq (6\epsilon)\frac{\theta}{\sqrt{2}} < 36\epsilon^2.$$

From Observation 2, the distance from each sample inside B to the tangent plane at p is at most $\frac{(6\epsilon+\epsilon^2)^2}{2} + \epsilon^2 < 20\epsilon^2$. Hence $(p-s_i)\cdot\vec{n} < 20\epsilon^2$. We can now write $P_{s_i}(x) = \phi(x) + \zeta_i$, where $|\zeta_i| \leq 56\epsilon^2 + 36|\phi(x)|\epsilon^2$. □

We now show that the value of $I(x)$ is mostly determined by the points inside $B_2(x)$ by proving results similar to Lemma 7 and Lemma 8 for a point x inside the τ-neighborhood.

Lemma 14. *For a point x in the τ-neighborhood,*

$$\frac{D_{\text{out}}(x)}{D_{\text{in}}(x)} < c_2.$$

Proof. For a point x inside the τ-neighborhood, $w_0 = \sqrt{(|\phi(x)|+\epsilon)^2+25\epsilon^2}$. Substituting this into Equation 3,

$$\frac{D_{\text{out}}(x)}{D_{\text{in}}(x)} \leq \frac{3200}{\epsilon^2}(w_0^2+\epsilon w_0+\epsilon^2)e^{-25}.$$

$\frac{D_{\text{out}}(x)}{D_{\text{in}}(x)}$ has the largest value when $\phi(x)$=τ and $w_o = \sqrt{34}\epsilon < 6\epsilon$. So

$$\frac{D_{\text{out}}(x)}{D_{\text{in}}(x)} < \frac{3200}{\epsilon^2}(43\epsilon^2)e^{-25} < c_2.$$ □

Lemma 8 is not true for x inside the τ-neighborhood, as $|N_{\text{in}}(x)|$ might be zero. However, we can prove an upper bound on $\frac{N_{\text{out}}(x)}{D(x)}$. The proof of this Lemma is exactly like the proof of Lemma 14.

Lemma 15. *For a point x inside the τ-neighborhood, $\frac{|N_{\text{out}}(x)|}{D(x)} < c_2\epsilon$.*

We begin by splitting the contributions to $\nabla I(x)$ in the following way: $\nabla I(x) = \nabla I_{\text{in}}(x) + \nabla I_{\text{out}}(x)$. Here,

$$\nabla I_{\text{in}}(x) = \frac{D_{\text{in}}(x)\nabla N_{\text{in}}(x) - N_{\text{in}}(x)\nabla D_{\text{in}}(x)}{D^2(x)}, \quad (6)$$

and

$$\begin{aligned}\nabla I_{\text{out}}(x) &= \frac{D_{\text{out}}(x)\nabla N_{\text{in}}(x)}{D^2(x)} + \frac{\nabla N_{\text{out}}(x)}{D(x)}\\ &\quad -\frac{N_{\text{out}}(x)\nabla D_{\text{in}}(x)}{D^2(x)} - \frac{N_{\text{in}}(x)\nabla D_{\text{out}}(x)}{D^2(x)}\\ &\quad -\frac{N_{\text{out}}(x)\nabla D_{\text{out}}(x)}{D^2(x)}. \quad (7)\end{aligned}$$

To show that the gradient of I is never zero inside the τ-neighborhood, we will prove a stronger result. For a point x in the τ-neighborhood, we show that $\nabla I(x)\cdot\vec{n} > 0$ where $\vec{n}$ is the normal of the point closest to x on the surface. In Section 6 we will use this result to show that U is homeomorphic to F.

The norm of the gradient of Gaussian weight functions decreases exponentially with distance. Using the proof technique of Lemma 8, we can obtain an upper bound on $\|\nabla N_{\text{out}}\|$ and $\|\nabla D_{\text{out}}\|$. Observation 16 summarizes the results.

Observation 16. *For a point x in the τ-neighborhood.*

1. $\left\|\frac{\nabla D_{\text{out}}(x)}{D(x)}\right\| < \frac{c_2}{\epsilon}$, *and*
2. $\left\|\frac{\nabla N_{\text{out}}(x)}{D(x)}\right\| < c_2$.

We now show that points outside $B_2(x)$ have little effect on $\nabla I(x)$ by proving an upper bound on $\|\nabla I_{\text{out}}(x)\|$.

Lemma 17. *For a point x in the τ-neighborhood, $\|\nabla I_{\text{out}}(x)\| < c_1$.*

Proof. We will compute the norm of each term in the expression for $\nabla I_{\text{out}}(x)$ given by Equation 7.

- $\left\| \frac{D_{\text{out}}(x)\nabla N_{\text{in}}(x)}{D^2(x)} \right\|$.

  We can write $\frac{\nabla N_{\text{in}}(x)}{D(x)}$ as

  $$\frac{\nabla N_{\text{in}}(x)}{D(x)} = \frac{\sum_{s_i \in B_2(x)} W_{s_i}(x)(n_i - \frac{2P_{s_i}(x)}{\epsilon^2}(x - s_i))}{\sum_{s_i} W_{s_i}(x)}.$$

  Clearly,

  $$\left\| \frac{\nabla N_{\text{in}}(x)}{D(x)} \right\| \leq \max_i \{\|n_i\| + \frac{|2P_{s_i}(x)|}{\epsilon^2}\|(x - s_i)\|\}.$$

  As x is inside the τ-neighborhood and s_i is inside $B_2(x)$, the point function $|P_{s_i}(x)| \leq \|(x - s_i)\| < 6\epsilon$. So $\left\| \frac{\nabla N_{\text{in}}(x)}{D(x)} \right\| < 73$. From Lemma 14, $\frac{D_{\text{out}}(x)}{D(x)} < c_2$.

  $$\left\| \frac{D_{\text{out}}(x)\nabla N_{\text{in}}(x)}{D^2(x)} \right\| < 73c_2. \tag{8}$$

- $\left\| \frac{\nabla N_{\text{out}}(x)}{D(x)} \right\|$

  From Observation 16,

  $$\left\| \frac{\nabla N_{\text{out}}(x)}{D(x)} \right\| < c_2. \tag{9}$$

- $\left\| \frac{N_{\text{out}}(x)\nabla D_{\text{in}}(x)}{D^2(x)} \right\|$

  $\frac{\nabla D_{\text{in}}(x)}{D(x)}$ can be written as

  $$\frac{\nabla D_{\text{in}}(x)}{D(x)} = \frac{\sum_{s_i \in B_2(x)} W_i(x)(-\frac{2}{\epsilon^2}(x - s_i))}{\sum_{s_i} e^{-\|x - s_i\|^2/\epsilon^2}}.$$

  As $\|x - s_i\| \leq 6\epsilon$, $\|\frac{\nabla D_{\text{in}}(x)}{D(x)}\| \leq \frac{12}{\epsilon}$. From Lemma 15, $\frac{N_{\text{out}}(x)}{D(x)} < c_2\epsilon$.

  $$\left\| \frac{N_{\text{out}}(x)\nabla D_{\text{in}}(x)}{D^2(x)} \right\| < 12c_2. \tag{10}$$

- $\left\| \frac{N_{\text{in}}(x)\nabla D_{\text{out}}(x)}{D^2(x)} \right\|$

  For any point x inside the τ-neighborhood, $|\frac{N_{\text{in}}(x)}{D(x)}| \leq \max\{P_{s_i}(x) | s_i \in B_2(x)\} \leq 6\epsilon$. From Observation 16, $\left\| \frac{\nabla D_{\text{out}}(x)}{D(x)} \right\| < \frac{c_2}{\epsilon}$.

  $$\left\| \frac{N_{\text{in}}(x)\nabla D_{\text{out}}(x)}{D^2(x)} \right\| < 6c_2. \tag{11}$$

- $\left\| \frac{N_{\text{out}}(x)\nabla D_{\text{out}}(x)}{D^2(x)} \right\|$

  From Observation 16, $\left\| \frac{\nabla D_{\text{out}}(x)}{D(x)} \right\| < \frac{c_2}{\epsilon}$. Combining this with the bound in Lemma 15,

  $$\left\| \frac{N_{\text{out}}(x)\nabla D_{\text{out}}(x)}{D^2(x)} \right\| < \frac{c_2}{\epsilon}(c_2\epsilon) < c_2^2. \tag{12}$$

Adding the norms of each term in the expression for $\nabla I_{\text{out}}(x)$ we get

$$\|\nabla I_{\text{out}}(x)\| < 93c_2 < c_1. \qquad \square$$

Theorem 18. *Let x be a point in the τ-neighborhood of F and let p be the point on F closest to x. Let $\vec{n}$ be the normal of p. Then for values of $\epsilon \leq 0.01$, $\vec{n} \cdot \nabla I(x) > 0$.*

Proof. From Lemma 17,

$$\vec{n} \cdot \nabla I_{\text{out}}(x) \leq \|\nabla I_{\text{out}}(x)\| < c_1.$$

We now consider the expression for $\nabla I_{\text{in}}(x)$.

$$\nabla I_{\text{in}}(x) = \frac{1}{D^2(x)} \sum_{s_i} \sum_{s_j} W_i(x)W_j(x)\{\vec{n}_i + \frac{2P_{s_i}(x)}{\epsilon^2}(s_i - s_j)\}.$$

The summation is over all samples $s_i, s_j \in B_2(x)$. From Observation 12, all samples in $B_2(x)$ are contained inside a ball of radius 6ϵ centered at p. So we can bound the difference between the point functions of samples inside $B_2(x)$ using Lemma 13.

The point function of each sample $s_i \in B_2(x)$ can be written as $P_{s_i}(x) = \phi(x) + \zeta_i$ where $|\zeta_i| < 56\epsilon^2 + 36\tau\epsilon^2 < 60\epsilon^2$. Let $C_{ij}(x) = W_i(x)W_j(x)$.

$$\begin{aligned}\nabla I_{\text{in}}(x) &= \frac{1}{D^2(x)} \sum_{s_i} \sum_{s_j} C_{ij}(x)(\vec{n}_i + \frac{2|\phi(x)|}{\epsilon^2}(s_i - s_j) \\ &\quad + \frac{2\zeta_i}{\epsilon^2}(s_i - s_j)) \\ &= \frac{1}{D^2(x)} \sum_{s_i} \sum_{s_j} C_{ij}(x)(\vec{n}_i + \frac{2\zeta_i}{\epsilon^2}(s_i - s_j)).\end{aligned}$$

From the above equation,

$$\vec{n} \cdot \nabla I_{\text{in}}(x) \geq \frac{\sum_{s_i} \sum_{s_j} C_{ij}(x)}{D^2(x)} \min_{ij}\{\vec{n} \cdot (\vec{n}_i + \frac{2\zeta_i}{\epsilon^2}(s_i - s_j))\}.$$

As we are summing over over all samples inside $B_2(x)$, $\sum_i \sum_j C_{ij}(x) = D_{\text{in}}^2(x)$. From Lemma 14, $\frac{D_{\text{in}}^2(x)}{D^2(x)} \geq (1 - c_1)^2$. Note that the samples inside $B_2(x)$ are in a ball of radius 6ϵ centered at p. Hence we can use Theorem 1 and Observation 2 to obtain an upper bound on the terms that appear in the above equation.

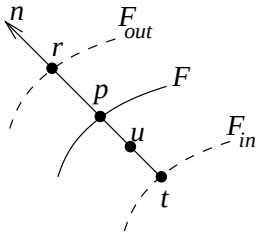

Figure 7: Points r, t are the closest points to p on the offset surfaces. The line segment rt intersects the zero set U at a unique point u.

From Theorem 1, the angle between $\vec{n}$ and $\vec{n}_i$ is less than 10ϵ. Hence $\vec{n} \cdot \vec{n}_i > \cos 10\epsilon$. From Observation 2, the distance from all samples inside $B_2(x)$ to the tangent plane at p is at most $\frac{(6\epsilon+\epsilon^2)^2}{2} + \epsilon^2$. Hence $\vec{n} \cdot (s_i - s_j) \leq 2(\frac{(6\epsilon+\epsilon^2)^2}{2} + \epsilon^2) < 40\epsilon^2$.

$$\begin{aligned}\vec{n} \cdot \nabla I(x) &\geq \vec{n} \cdot \nabla I_{\text{in}}(x) - \|\nabla I_{\text{out}}(x)\| \\ &\geq (1-c_1)^2(\cos(10\epsilon) - \\ &\quad \max\{\frac{2\zeta_i}{\epsilon^2}|\vec{n} \cdot (s_i - s_j)|\}) - c_1 \\ &\geq (1-c_1)^2(\cos(10\epsilon) - 4800\epsilon^2) - c_1.\end{aligned}$$

It is easy to verify that $\vec{n} \cdot \nabla I(x) > 0$ for values of $\epsilon \leq 0.01$. □

Theorem 18 also proves that the gradient can never be zero inside the τ-neighborhood. From Theorem 9, the zero set of I is inside the τ-neighborhood of F. Hence from the implicit function theorem [7], zero is a *regular* value of I and the zero set U is a compact, two-dimensional manifold.

The normal of the reconstructed surface at a point $u \in U$ is determined by the gradient of the implicit function at u, $\vec{n}_u = \frac{\nabla I(u)}{\|\nabla I(u)\|}$. Using Theorem 18, we can bound the angle between $\vec{n}_u$ and the normal of the point closest to u in F.

Theorem 19. *Let u be a point on the reconstructed surface U whose closest point on F is p. Let $\vec{n}_u$ be the normal of U at point u and let $\vec{n}$ be the normal of F at point p. An upper bound on the angle θ between $\vec{n}_u$ and $\vec{n}$ is given by,*

$$\cos\theta \geq \frac{(1-c_1)^2(\cos(10\epsilon) - 4800\epsilon^2) - c_1}{1 + 2400\epsilon + c_1}.$$

6 Topological Properties

We now use the results in Section 5 to define a homeomorphism between F and U. As F and U are compact, a one-to-one, onto, and continuous function from U to F defines a homeomorphism.

Definition: Let $\Gamma : \mathbb{R}^3 \rightarrow F$ map each point $q \in \mathbb{R}^3$ to the closest point of F.

Theorem 20. *The restriction of Γ to U is a homeomorphism from U to F.*

Proof. The discontinuities of Γ are the points on the medial axis of F. As U is constrained to be inside the τ-neighborhood of F, the restriction of Γ to U is continuous.

Now we show that Γ is one-to-one. Let p be a point on F and let $\vec{n}$ be the normal at p as shown in Figure 7. Consider the line segment parallel to $\vec{n}$ from r to t. At each point $y \in rt$, $\nabla I(y) \cdot \vec{n} > 0$ from Theorem 18. So the function $I(x)$ is monotonically decreasing from r to t and there is a unique point u on rt where $I(u) = 0$. Assume there is another point $v \in U$ for which $\Gamma(v) = x$. The point v has to be outside the segment rt and the distance from v to its closest point on F is greater than τ. This contradicts Theorem 10.

Finally we need to show that Γ is onto. As Γ maps closed components of U onto closed components of F in a continuous manner, $\Gamma(U)$ should consist of a set of closed connected components. Consider the point p in Figure 7. Assume that $q = \Gamma(u)$ is not in the same component of F as p. Let B_u be the ball of radius τ centered at u that intersects two components of F, one containing point p and one containing point q. Boissonnat and Cazals [9] (Proposition 12) show that any ball whose intersection with F is not a topological disc contains a point of the medial axis of F. Since point p is inside the ball B_u that contains a point of the medial axis, $\text{lfs}(p) \leq 2\tau$. Recall that $\tau = 2\epsilon$ and that our sampling conditions require $\epsilon \leq 0.01$. Hence, $\text{lfs}(p) \leq 2\tau \leq 0.04$. This violates our assumption that $\text{lfs}(p) \geq 1$. □

7 Discussion

One disadvantage of our algorithm is that it requires sample normals. However, approximate sample normals can be easily obtained for laser range data by triangulating the range images. Each sample normal can be oriented using the location of the range scanner. When oriented normals are unavailable, the absolute distance to the tangent plane at each sample can be used instead of the signed distance as a point function to define a new function $I_u(x)$. The zero set of this function is hard to analyze as its gradient is not smooth near the sample points. However, the results in this paper can be easily extended to show that the τ-level set of $I_u(x)$ consists of two components on each side of the surface, each homeomorphic to F.

Our sampling requirements are determined by the smallest local feature size of a point on F. Recall that the width of the Gaussian functions used in our algorithm depends on the smallest local feature size. When sampling density is proportional to the local feature size, the width of the Gaussian weight functions might be much smaller than the spacing between sample points in areas of the surface with large local feature size. As a result, the reconstructed surface will be noisy and might have the wrong topology. One solution is to make the width of the Gaussian weight functions

proportional to the spacing between sample points. We are currently working on extending the MLS construction and our proofs to deal with adaptively sampled surfaces.

The implicit surface we construct in this paper only passes near the sample points, but we can construct a surface that interpolates the sample points with weight functions such as $W_s(x) = \frac{e^{-\|x-s\|^2}}{\|x-s\|^2}$, that are infinite at the sample points. We can prove that the zero set is restricted to the τ-neighborhood when this weight function is used, but, we could not prove results about the gradient approximations.

Acknowledgments

I would like to thank Nina Amenta, James O'Brien and my advisor Jonathan Shewchuk for helpful comments. I would also like to thank François Labelle for reading the proofs and for pointing out an error in an earlier version of the paper.

References

[1] A. ADAMSON AND M. ALEXA, *Approximating and Intersecting Surfaces from Points*, in Proceedings of the Eurographics Symposium on Geometry Processing, Eurographics Association, 2003, pp. 230–239.

[2] M. ALEXA, J. BEHR, D. COHEN-OR, S. FLEISHMAN, D. LEVIN, AND C. T. SILVA, *Computing and Rendering Point Set Surfaces*, IEEE Transactions on Visualization and Computer Graphics, 9 (2003), pp. 3–15.

[3] N. AMENTA AND M. BERN, *Surface Reconstruction by Voronoi Filtering*, Discrete & Computational Geometry, 22 (1999), pp. 481–504.

[4] N. AMENTA, S. CHOI, T. K. DEY, AND N. LEEKHA, *A Simple Algorithm for Homeomorphic Surface Reconstruction*, International Journal of Computational Geometry and Applications, 12 (2002), pp. 125–141.

[5] N. AMENTA, S. CHOI, AND R. KOLLURI, *The Power Crust*, in Proceedings of the Sixth Symposium on Solid Modeling, Association for Computing Machinery, 2001, pp. 249–260.

[6] N. AMENTA AND Y. KIL, *Defining Point-Set Surfaces*, ACM Transactions on Graphics, 23 (2004), pp. 264–270.

[7] J. BLOOMENTHAL, ed., *Introduction to Implicit Surfaces*, Morgan Kaufman, 1997.

[8] J.-D. BOISSONNAT AND F. CAZALS, *Smooth Surface Reconstruction via Natural Neighbour Interpolation of Distance Functions*, in Proceedings of the Sixteenth Annual Symposium on Computational geometry, ACM, 2000, pp. 223–232.

[9] ———, *Natural Neighbor Coordinates of Points on a Surface*, Computational Geometry Theory and Applications, 19 (2001), pp. 155–173.

[10] J.-D. BOISSONNAT, D. COHEN-STEINER, AND G. VEGTER, *Isotopic Implicit Surface Meshing*, in Proceedings of the Thirty-Sixth Annual ACM Symposium on Theory of Computing, 2004, pp. 301–309.

[11] J. D. BOISSONNAT AND S. OUDOT, *Provably Good Surface Sampling and Approximation*, in Proceedings of the Eurographics Symposium on Geometry Processing, Eurographics Association, 2003, pp. 9–18.

[12] J. C. CARR, R. K. BEATSON, J. B. CHERRIE, T. J. MITCHELL, W. R. FRIGHT, B. C. MCCALLUM, AND T. R. EVANS, *Reconstruction and Representation of 3D Objects with Radial Basis Functions*, in Computer Graphics (SIGGRAPH 2001 Proceedings), Aug. 2001, pp. 67–76.

[13] B. CURLESS AND M. LEVOY, *A Volumetric Method for Building Complex Models from Range Images*, in Computer Graphics (SIGGRAPH '96 Proceedings), 1996, pp. 303–312.

[14] T. K. DEY AND S. GOSWAMI, *Provable Surface Reconstruction from Noisy Samples*, in Proceedings of the Twentieth Annual Symposium on Computational Geometry, Brooklyn, New York, June 2004, Association for Computing Machinery.

[15] S. FLEISHMAN, M. ALEXA, D. COHEN-OR, AND C. T. SILVA, *Progressive Point Set Surfaces*, ACM Transactions on Computer Graphics, 22 (2003).

[16] H. HOPPE, T. DEROSE, T. DUCHAMP, J. MCDONALD, AND W. STUETZLE, *Surface Reconstruction from Unorganized Points*, in Computer Graphics (SIGGRAPH '92 Proceedings), 1992, pp. 71–78.

[17] D. LEVIN, *Mesh-Independent Surface Interpolation*, in Geometric Modeling for Scientific Visualization, G. Brunett, B. Hamann, K. Mueller, and L. Linsen, eds., Springer-Verlag, 2003.

[18] M. LEVOY, K. PULLI, B. CURLESS, S. RUSINKIEWICZ, D. KOLLER, L. PEREIRA, M. GINZTON, S. ANDERSON, J. DAVIS, J. GINSBERG, J. SHADE, AND D. FULK, *The Digital Michelangelo Project: 3D Scanning of Large Statues*, in Computer Graphics (SIGGRAPH 2000 Proceedings), 2000, pp. 131–144.

[19] W. E. LORENSEN AND H. E. CLINE, *Marching Cubes: A High Resolution 3D Surface Construction Algorithm*, in Computer Graphics (SIGGRAPH '87 Proceedings), July 1987, pp. 163–170.

[20] N. J. MITRA, N. GELFAND, H. POTTMANN, AND L. GUIBAS, *Registration of Point Cloud Data from a Geometric Optimization Perspective*, in Symposium on Geometry Processing, 2004.

[21] N. J. MITRA, A. NGUYEN, AND L. GUIBAS, *Estimating Surface Normals in Noisy Point Cloud Data*, International Journal of Computational Geometry and Applications, 14 (2004), pp. 261–276.

[22] Y. OHTAKE, A. BELYAEV, M. ALEXA, G. TURK, AND H.-P. SEIDEL, *Multi-Level Partition of Unity Implicits*, ACM Transactions on Graphics, 22 (2003), pp. 463–470.

[23] S. OSHER AND R. FEDKIW, *The Level Set Method and Dynamic Implicit Surfaces*, Springer-Verlag, New York, 2003.

[24] M. PAULY, R. KEISER, L. P. KOBBELT, AND M. GROSS, *Shape Modeling with Point-Sampled Geometry*, ACM Trans. Graph., 22 (2003), pp. 641–650.

[25] C. SHEN, J. F. O'BRIEN, AND J. R. SHEWCHUK, *Interpolating and Approximating Implicit Surfaces from Polygon Soup*, ACM Transactions on Graphics, 23 (2004), pp. 896–904.

[26] G. TURK AND J. O'BRIEN, *Shape Transformation Using Variational Implicit Functions*, in Computer Graphics (SIGGRAPH '99 Proceedings), 1999, pp. 335–342.

[27] H.-K. ZHAO, S. OSHER, AND R. FEDKIW, *Fast Surface Reconstruction Using the Level Set Method*, in First IEEE Workshop on Variational and Level Set Methods, 2001, pp. 194–202.